16th World Conference on Earthquake Engineering, 16WCEE 2017

Santiago Chile, January 9th to 13th 2017

Paper N° 111

Registration Code: S- R1463431150

Simulation analysis of earthquake damaged reinforced concrete beams under fire

Bo Wen[1], Ditao Niu[2], Bao Wang[3]

[1] *Professor, Xi'an University of Architecture & Technology, wenbo_mail@163.com*
[2] *Professor, Xi'an University of Architecture & Technology, niuditao@163.com*
[3] *Postgraduate Student, Xi'an University of Architecture & Technology, 304310717@qq.com*

Abstract

Geometrical damaged models of earthquake damaged reinforced concrete beams under post-earthquake fire are established and simulation analysis of thermal fields are performed. Based on a large number of earthquake damage examples, the geometrical damage of reinforced concrete beams are defined as cracks and spalling. Based on this information, some geometrical parameters are proposed to form the damage model of RC beams in ABAQUS. The thermal fields of reinforced concrete beams under post-earthquake fire are calculated in the end. It is found that cracks and spalling as the geometrical parameters for earthquake damaged beams is reasonable. Meanwhile, the locations of cracks and spalling affect the thermal fields of post-earthquake fire reinforced concrete beams dramatically.

Keywords: Post-earthquake fire, reinforced concrete beams, cracks, spalling, thermal field analysis

1. Introduction

According to statistics from earthquake damage, it is found that post-earthquake fires (PEF) usually occur with high probability and the loss caused by PEF is even more severe than the loss from the earthquake itself [1-3]. Thus studying the mechanical properties of structures under PEF, although complex and difficult to predict, is extremely important [4]. In the February 4, 1975, China Haicheng (M7.3) earthquake, there were more than 700 deaths and more than 7,000 injured by PEF [5]. In January 17, 1995, after the Kobe earthquake in Japan, in addition to a large number of casualties caused by the housing collapse, the most serious disaster was caused by PEF and more than 500 people died from PEF [6]. In the September 21, 1999 Chi-Chi earthquake in Taiwan (M7.3), from the survey in the most severely affected seven counties, there were 161 PEF disasters in seven days [7]. These real life examples from so many earthquakes shows the importance of PEF research and more attention should be paid to studying this area not only to discover the potential for severe structural damage during a PEF, but for the development of more strict design requirements to alleviate this potential PEF hazard to structures.

Many scholars have focused their research on the fire resistance of structures under PEF and have received a great deal of encouraging results. Data obtained from PEF in the Kanto earthquake regarding wooden structures was analyzed by Kawasumi et al. [8] They documented the relationship of fire ratio and collapse ratio of wooden structures. Keisuke et al. [9] created a fire spread model of a city based on its physical structures. According to the fire statistics by the US Geological Survey [10], the relationship of fire ratio and earthquake intensity was recognized. Pucinotti et al. [11] studied the earthquake damage to steel frames with refractory material and, using numerical simulation, compared the thermal field of damaged joints and undamaged joints. The results showed that the destruction of the beam-column joints makes thermal conductivity higher than that of undamaged joints. Oreste et al. [12] performed a seismic test of four beam-column joint specimens and then applied the fire load on them. The results indicated that the joint could withstand fire load for about 15 minutes, and the performance of the precast joint was better than that of the composite joint. Wu et al. [13] had done a great deal of research on the influence of heat conduction on the cracks of concrete structures. In their experiment, ten concrete specimens (nine with pre-made cracks of varying widths and one without cracks) had been tested in fire to investigate the effect of cracks on temperature distributions of concrete members subjected to PEF. From experimental investigations and numerical calculations, it was found that the temperatures measured on the surface of the concrete specimens with the pre-made crack were generally lower than those on the central cross section of the non-cracked control specimen. When the crack is less than 3 mm wide, the influence of the crack width on the temperature distributions is negligible, As the crack width increases, the temperatures rise slightly.

Although there has been much research about fire resistance, most of which are focused on the performance of steel structures while only a small part of which is involved in the mechanism performance of RC structures or RC elements under PEF. Because earthquakes damage the RC structures or elements before a fire, the mechanical properties of earthquake damaged RC structures or elements under high temperature must be different than those of undamaged RC structures or elements. Therefore, it is necessary to continue to research more aspects of this area. Damaged RC beams were categorized as to the extent of the crack and spalling damage first, then the model with two geometrical parameters comparing crack depth and relative spalling width were investigated. Based on numerical simulation in ABAQUS, the calculated results regarding thermal field and bearing capacity of the RC beams under PEF were analyzed.

2. Mechanical parameters of concrete and reinforcement under high temperatures

2.1 Mechanical parameters of concrete under high temperature

From the European Code EC2 (2005) [14], thermal conductivity of concrete is shown in Eq.(1) and Eq.(2), which are the upper and lower limit of thermal conductivity separately, taking the average value of the two equations as the basis for the thermal analysis of concrete.

Upper limit of the equation:

$$\lambda_c = 2 - 0.2451 \times (\frac{T}{100}) + 0.0107 \times (\frac{T}{100})^2 \quad 20℃ \le T \le 1200℃ \tag{1}$$

Lower limit of the equation:

$$\lambda_c = 1.36 - 0.136 \times (\frac{T}{100}) + 0.0057 \times (\frac{T}{100})^2 \quad 20℃ \le T \le 1200℃ \tag{2}$$

Where λc is thermal conductivity of concrete.

From the European Code EC4 (2005) [15] , the heat capacity of concrete quality and the coefficient of thermal expansion are shown in Eq.(3) and Eq.(4). The density of concrete ρc is taken as a constant value 2400 *kg/m*^{3}.

$$C_c = \begin{cases} 900 & 20℃ \le T_s \le 100℃ \\ 900 + (T - 100) & 100℃ < T_s \le 200℃ \\ 1000 + (T - 200)/2 & 200℃ < T_s \le 400℃ \\ 1100 & 400℃ < T_s \le 1200℃ \end{cases} \tag{3}$$

$$\Delta l / l = \begin{cases} -1.8 \times 10^{-4} + 9 \times 10^{-6} T + 2.3 \times 10^{-11} T^3 & 20℃ \le T_s \le 700℃ \\ 14 \times 10^{-3} & 700℃ < T_s \le 1200℃ \end{cases} \tag{4}$$

Where Cc is heat capacity of concrete quality, $l\Delta$ is the coefficient of thermal expansion of concrete.

The elastic modulus of concrete E_c^T and the compressive strength f_{cu}^T at high temperature are chosen from literature [16] which are shown in Eq. (5) and Eq. (6) respectively.

$$E_c^T / E_c = 0.83 - 0.0011T \quad 60℃ \le \mathrm{T} \le 700℃ \tag{5}$$

$$\frac{f_{cu}^T}{f_{cu}} = \frac{1}{1 + 16(T/1000)^{6.3}} \tag{6}$$

Where Ec and fcu are the elastic modulus and the compressive strength under common room temperature, respectively..

The relationship of concrete stress-strain is shown in Equation (7).

$$y = \begin{cases} 2.2x - 1.4x^2 + 0.2x^3 & x < 1 \\ \dfrac{x}{0.8(x-1)^2 + x} & x \ge 1 \end{cases} \tag{7}$$

Where, $\mathrm{y} = \frac{\sigma}{f_c^T}$, $x = \frac{\varepsilon}{\varepsilon_p^T}$, $\frac{\varepsilon_p^T}{\varepsilon_p} = 1 + 5(\frac{T}{1000})^{1.7}$, f_c^T and ε_p^T are the compressive strength and peak strain of ordinary concrete under high temperature separately.

2.2 Mechanical parameters of Reinforcement under high temperature

The density, elasticity modulus and yield strength of reinforcement in thermal analysis are chosen from literature [17] shown in Eq.8 and Eq.9. The density of steel ρs is 7800 *kg/m*^{3}.

$$E_s^T = f_y^T / \varepsilon_y^T \tag{8}$$

$$\frac{f_y^T}{f_y} = \frac{1}{1+24(\frac{T}{1000})^{4.5}} \tag{9}$$

Where T is the temperature, E_s^T is the elasticity modulus, f_y^T is the yield strength, f_y^T is the tensile strength.

2.3 The basic assumptions of temperature field analysis

In order to simulate conditions of the concrete beams under high temperature, some basic assumptions are proposed in temperature field analysis [18-19].

(1) ISO 834 standard heating curve is used as input heat wave.

(2) Room temperature air is uniform.

(3) RC beams are considered as a homogeneous material, whose thermal conductivity is uniform and isotropic.

(4) The thermal field contribution of internal reinforcement and bond slip between reinforcement and concrete is not addressed. This would be a good area for deeper study.

3 Calculation model of damaged RC beams

3.1 Damaged survey of RC beams in earthquake

Even though the damage to RC structures is different with varying earthquake intensities, some rules are useful to follow using a statistical survey of the damage to RC structures in some previous earthquakes. Table 1 shows the percentage of relative damage to RC structures in selected earthquakes. 'Slight damage' means there are some small local cracks on the elements and rebar is not exposed, 'moderate damage' means there is some local spalling of the concrete cover and reinforcement is exposed but not buckling.

Table 1 Statistics showing percentage of RC structures damaged

Earthquake	Intensity of earthquake	No damage	Slight damage	Moderate damage	Severe damage	Collapse
Lancang, China, 1988 [20]	M7.6	12.50%	35.20%	29.20%	8.30%	14.50%
Southern Hyogo, Japan, 1995 [21]	M7.2	65.25%		12.60%	22.15%	
Guye, China, 1998 [22]	M4.7	93.24%	4.05%	2.70%	0%	0%
Wenchuan, China, 2008 [23]	M8.0	55.74%		34.43%	9.80%	
Yingjiang, China, 2011 [24]	M5.8	30.04%	27.88%	19.88%	13.83%	8.37%

According to the statistical data from Table 1, most structures fit under the categories of slight or moderate damage by crack (shown in Fig.1) and spalling (shown in Fig.2).

Fig.1 Crack of beam

Fig.2 Spalling of beam

3.2 Geometrical parameters of earthquake damaged beams

In order to measure the earthquake damage consistently, crack length, crack depth , spalling width and spalling length are usually proposed as geometrical parameters in earthquake damage elements. Comparing the parameters of the different damage elements, the relative crack length $\bar{l}/h$ is defined as the ratio of crack length $\bar{l}$ and cross-section height h, the relative crack depth $\bar{d}/h$ is defined as the ratio of crack depth $\bar{d}$ and section height h, the relative spalling width $\bar{b}/h$ is defined as the ratio of spalling width $\bar{b}$ and section height h, the relative spalling height $\bar{h}/h$ is defined as the ratio of spalling height $\bar{h}$ and height h. From most earthquake examples, it is usually found that the crack length and spalling length have little variation when compared with each other, therefore, only relative crack depth and relative spalling width are used in the following analysis.

3.3 Earthquake damaged beam model

For investigating the rule of geometrical parameters of earthquake damaged beams in detail, the models of crack beam and spalling beam are established separately. It should be mentioned that the crack model and spalling model established in this paper are based on the assumption that RC beams are suffered by slight damage and moderate damage because the most possibility damage occurred in earthquakes are these two types shown in Table 1. For the limitation of the scope of the paper, the numerical simulation of thermal analysis and moment capacity of PEF beams are focused on the slight damaged and moderate damaged beams.

Meanwhile, from literatures [13], [14] and [16] etc., it's shown that fire effect is more severe in isolated beam than in that of flange beam. In order to study the fire performance of PEF RC beams clearly, for the primary research, the isolated beams are modeled in this paper without considering the support of floor slab.

3.3.1 Crack beam model

Looking at the data from actual earthquakes and the literature [25], the relative crack length $\bar{l}/h$ will be defined as 0.25 (B1), 0.5 (B2) and 1.0 (B3), which are shown in Fig.3. The crack beam with reinforcement is shown in Fig.4. Based on the assumptions and relative crack depth of damaged beams, the calculated models of crack beams are established in ABAQUS [26] which are shown in Fig.5.

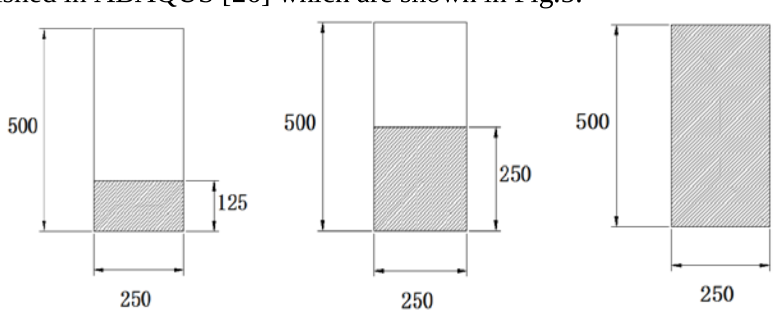

(a) B1 (b) B2 (c) B3

Fig.3 Section of crack beams

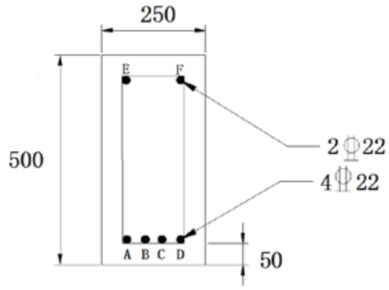

Fig.4 Reinforcement of beam

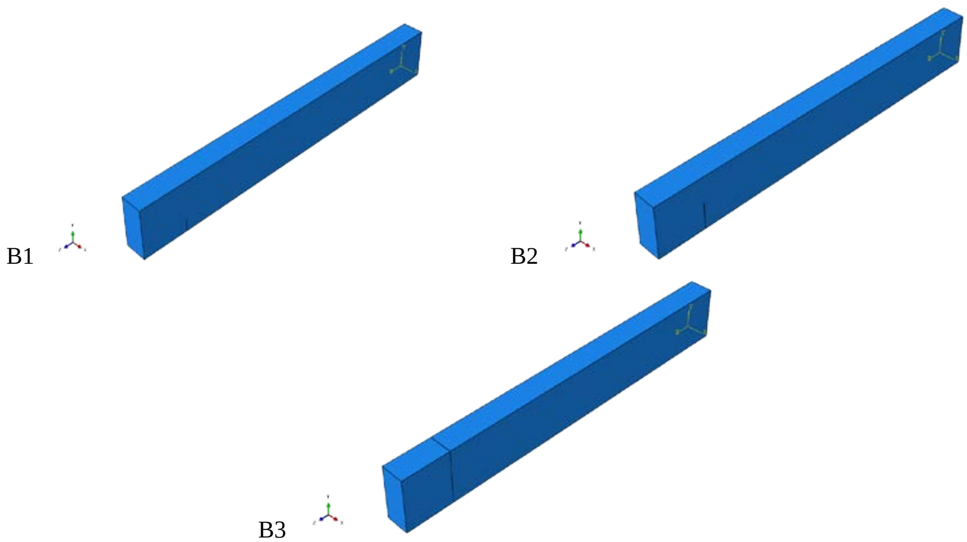

Fig.5 Finite element model of crack beams

3.3.2 Spalling beam model

Like crack beams, the geometrical damage dimensions of spalling beams are usually summarized from actual earthquake damage examples. When spalling occurs at both the upper edge and lower edge of beam, it is designated as L1 spalling. The spalling at the upper edge of beam is L2 and spalling at lower ends of the beam is L3. The beam without spalling is L0. The cross-section of spalling beams are shown in Fig.6. From earthquake examples and literature, where the concrete near the edges of beams are spalled completely, the relative spalling width and height is designated asn1.0 and 0.4, respectively. The spalling beam length L is 4.0m and the thickness of the concrete cover is 25mm. The calculated models of spalling beams are established in ABAQUS which are shown in Fig.7.

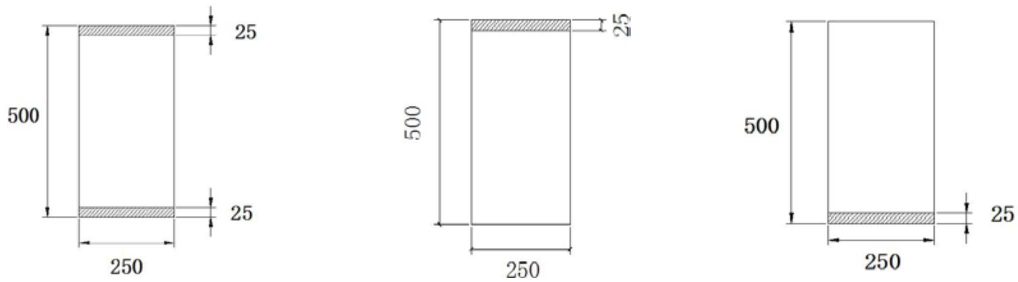

(a) L1 (b) L2 (c) L3

Fig.6 Section of spalling beams

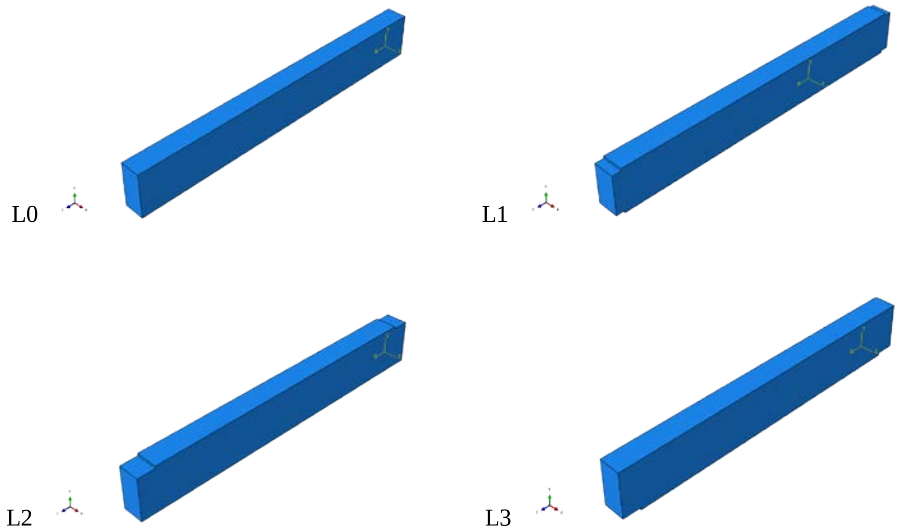

Fig.7 Finite element model of spalling beams

4 Thermal field analysis of PEF RC beams

4.1 Parameters in heating propagation

ABAQUS software is used in this paper for thermal field analysis and bearing capacity calculation of the PEF RC beams, in which the boundary conditions of heating convection and radiation are selected from European Code EC2 and EC4 shown in Eq.1 to Eq.4, in which the convective heat transfer coefficient is 25W/(m • K), integrated radiation coefficient is 0.7, air temperature is taken as 20℃ and ISO 834 standard temperature curve is used as heating curve. Absolute zero is defined as -273℃ and Stephen - Boltzmann constant is taken as 5.67×10-8. In ABAQUS, DC3D8 is used as thermal analysis unit and all these heating propagation parameters are installed in CAE file.

4.2 Verification of model validity

In order to verify the validity of using ABAQUS software to simulate thermal tests on PEF RC beams under high temperature, the test temperature values of RC beams from literature [27] are numerically simulated. The software calculated and literature derived test points are shown in Fig.8 (a) and Fig.8 (b) respectively. The relative curves of the test and calculated values are shown in Fig.8 (c). The closely correlated data from the calculated model and field test results from the literature confirms the validity of using the ABAQUS software to simulate future thermal tests. Therefore, it is reasonable to use ABAQUS models to study the thermal fields of PEF RC beams.

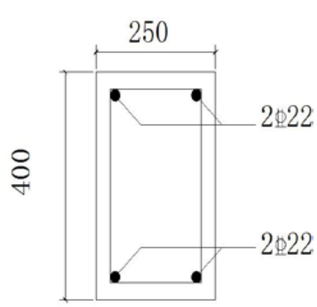

(a) Software calculated values

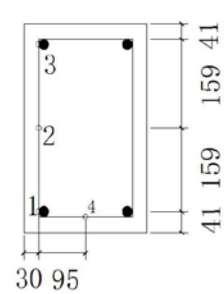

(b) Literature derived test points

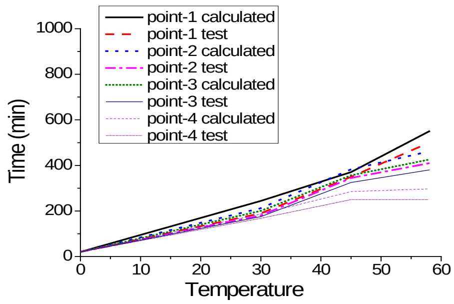

(c) Graph of calculated and test points

Fig.8 Temperature curves of software calculations and field tests

4.3 Thermal field analysis of PEF RC beams

4.3.1 Thermal field contours of crack beams

The thermal fields of PEF RC beams are calculated in ABAQUS. The ISO834 is selected as the standard heating curve. The heating time is from zero to 21,600 seconds. Three sides of the beam are exposed to fire which is shown in Fig.9. The sectional thermal field contours and the longitudinal thermal field contours of PEF RC crack beams are shown in Fig.10 and Fig.11 respectively.

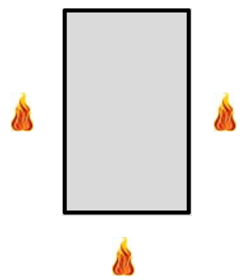

Fig.9 PEF RC beams exposed to fire

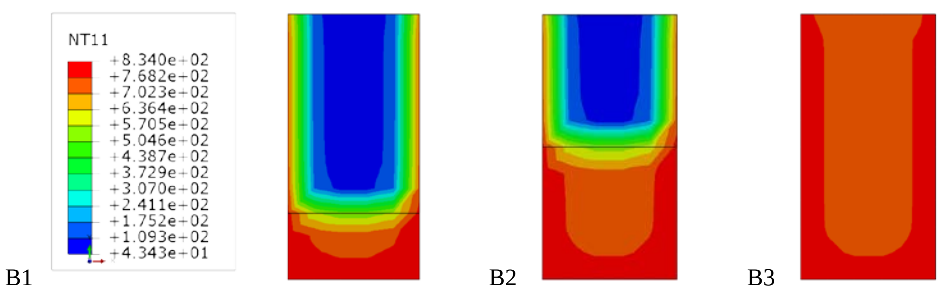

(a) t=1,800s

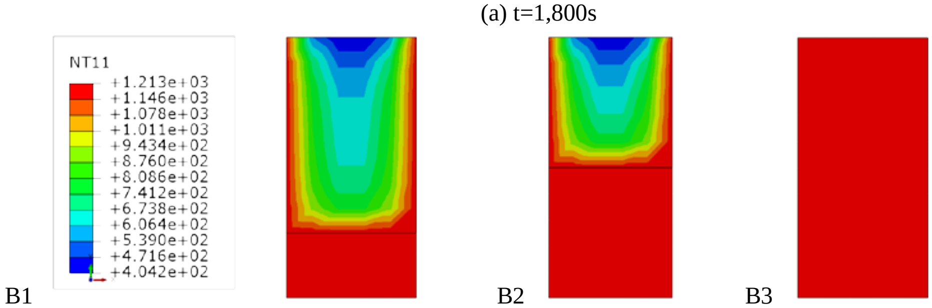

(b) t=21,600s

Fig.10 Sectional thermal field of crack beams

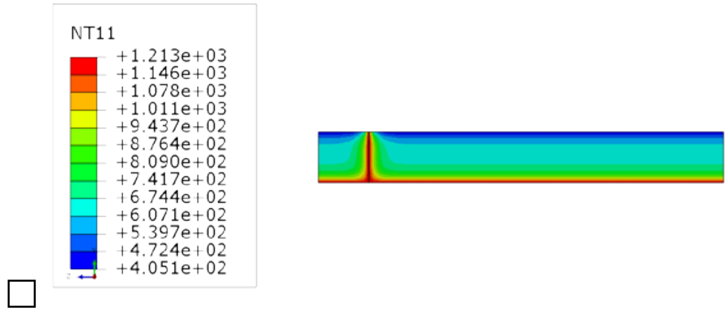

Fig.11 Longitudinal thermal field of crack beams

From Fig.10 and Fig.11, it is clear that the thermal field distribution of the cracks under high temperature are in mostly a 'U' shape and the depth of the cracks has a great effect on the thermal field of PEF RC crack beams. When the crack depth increases, the temperatures around the crack increase as well. The greater the crack depth, the greater the difference in temperature between the crack surface and inside the beam at the same height.

4.3.2 Thermal field contours of spalling beams

The temperature field contours of spalling beams from zero to 21,600 seconds are shown in Fig.12. This indicates that the overall temperature distribution of different spalling beams are similar. As the fire time increases, the thermal field of spalling beams is also gradually changing.

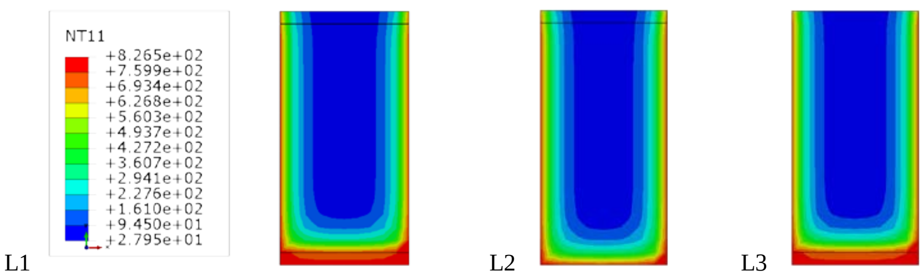

(a) t=1,800s

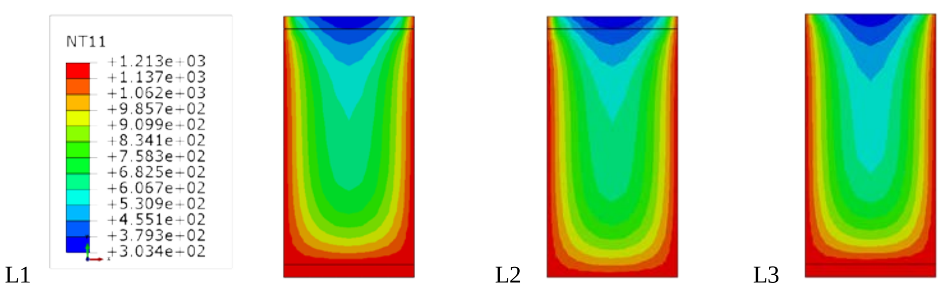

(b) t=21,600s

Fig.12 Thermal field contours of spalling beams

Fig.12, shows that spalling has obvious effects on the thermal field of the beam. The shape of thermal field contours on the three sides exposed to the fire is increasing as the temperature rises. When the temperature is lower, the contours have a 'U' shape which indicates the temperature difference between different spalling beams isn't obvious and the temperature area of the spalling beams at the bottom is lower than that of the same location of the undamaged beams. As the heating time increases, the inner temperature of the spalling beam increases as well. The thermal field contours of spalling beams changes from a 'U' shape to a 'V' shape, which indicates that the lower temperature area in the core of the concrete moves from the back side to the top side of the beam section. Interestingly, the field distribution of different beams is very similar to each other, which means the spalling location has little effect on the thermal field of beams.

5 Conclusions

It is known from earthquake examples that post-earthquake fire poses a severe threat to the damaged RC elements. Current studies have include very little about the fire resistance of PEF RC elements. For this reason, the thermal field and bending capacity of PEF RC beams under high temperature are numerically studied in this paper and the following conclusions can be drawn:

(1) From real earthquake examples and literature, the geometrically damaged types of PEF RC beams can be divided into two types: crack and spalling. The damaged parameters are usually defined as crack length, crack depth, spalling width and spalling length.

(2) For the crack beams, the crack has the greatest effect on the thermal field under high temperature. The deeper the crack, the higher the temperature near the crack resulting in a “U” shaped contour. The most significant change of the contour occurs around the crack.

(3) The thermal field of the spalling beam is limited by the location of the spalling. The spalling at the bottom edge of the beam has more effect on the thermal field than that of an upper section of a spalling beam. With temperature increasing, the low-temperature region moves from the bottom back to the upper edge and thus the shape of the contour changes from "U" to "V".

Acknowledgements

This research is financially supported by National Natural Science Foundation of China (No.51578450, in China), South China University of Technology Open Project (No.2013KA04, in China), International cooperation projects of Shaanxi Province (No. 2013KW23-02), and Shaanxi Provincial Department of Housing and Urban-Rural Development Science & Technology Project (No. 2015-23, in China).

References

[1] Berkeley Seismological Laboratory. Where can I learn more about 1906 Earthquake? http://www.seismo.berkeley.edu/seismo/hayward/seismicity.hist_1906.html, 2003-03-01.

[2] Oppenheim, I. Modeling Earthquake-Induced Fire Losses. Proc. 8th World conf. on Earthquake Engineering, vol: VIII, 1984, pp: 777-784.

[3] Dahlmann J, Joseph S. The Great Tokyo Earthquake September 1, 1923: Experiences and Impressions of an Eye-Witness. The America Press, 1924.

[4] Mohammadi J, Alyasin S, Bak D. Analysis of post-earthquake fire hazard. Proc. 10th World Conf. on Earthquake Engineering, vol:II, 1992, pp:5983-5988.

[5] Li G. Q., Wu B., Han L. H. Development of the research on fire-resistance of structures. Progress in steel building structures. 2006, 8(1): 1-13. (in Chinese)

[6] Scawthorn C. Fires following the Northridge and Kobe earthquakes. The Thirteenth Meeting of the UJNR Panel on Fire Research and Safety. 1996, 2: 337-345.

[7] Li Z.,Wang X. Q., , Wang C. Study on Death Rate of Chi-Chi Earthquake. North china earthquake sciences, 2010, 28(9): 1-5.

[8] Kawasumi M. Urban post-earthquake fires in Japan. Proceedings U.S.-Japan Workshop on Urban Earthquake Hazards Reduction, 1985: 121-133.

[9] Keisuke H, Takeyoshi T. A physically-based model for urban fire spread. First Safety Science - Proceedings of the Seven International Symposiums. 2002: 129-140.

[10] United States Geological Survey (USGS). The Loma Prieta, California, Earthquake of October 17, 1989-Fire, Police, Transportation, and Hazardous Materials. U. S. Government Office, Washington, Paper: 1553, 1994.

[11] Pucinotti R, Bursi O, Demonceau J. Post-earthquake fire and seismic performance of welded steel concrete composite beam-to-column joints. Journal of Constructional Steel Research, 2011, 67:1358-1375.

[12] Oreste S, Fabio F, Raffaele P. Seismic-induced fire analysis of steel-concrete composite beam-to-column joints: bolted solutions. International Conference on Composite Construction in Steel and Concrete Composite Construction in steel and Concrete, 2008, IV, 494-505.

[13] Wu, B., Xiong, W., Wen, B. Thermal fields of cracked concrete members in fire. Fire Safety Journal, 2014, 66, 15-24.

[14] Eurocode 2. Design of Concrete Structure (Part 1-2: General Rules-Structural Fire Design), BSEN1992-1-2, British Standards Institution, London, 2005, 23-28.

[15] Eurocode 4. Design of composite steel and concrete structures (Part 1-2: General rules-Structural Fire Design), EN1994-1-2, Brussels, European committee for Standardization, 2005, 36-40.

[16] Guo, Z. H. Principle of reinforced concrete. China: Beijing, Tsinghua university press, 1999, 67-78. (in Chinese)

[17] Guo, Z.H., Shi, X.D. Experimental and Calculation of Reinforced Concrete at Elevated Temperatures, Tsinghua University Press, Beijing, 2011:311 (in Chinese).

[18] ISO, Fire Resistance Tests: Elements of Building Construction. ISO834, Geneva, 1999.

[19] Behrouz, B., Hamid, R Performance of reinforced concrete structures subjected to fire following earthquake. European Journal of Environmental and civil Engineering, 2013, 17(4): 270-292.

[20] Na X. Q., Zhou X. Y. Investigation of Earthquake Damages of Building Structures in Lancang and Gengma of Yunnan province. Journal of Building Structures, 1991, 12(4): 62-71. (in Chinese)

[21] Cui H. C. Summary of damage over southern Japan Hyogo Earthquake. Journal of Building Structures .1996,17 (1): 2-13. (in Chinese)

[22] Su Y. P., Wang S. J. Investigation and analysis to building damages caused by the Guye M4.7 earthquake occurred on April, 14 of 1998. Hebei Metallurgy. 1998, 104-107:78-83. (in Chinese)

[23] Wu Z. B., Zhou X. X., Xie W., et al. Statistics of Wenchuan Earthquake investigation and some ideas on seismic design of buildings. Building Structure. 2010, 6: 144-148. (in Chinese)

[24] Zhou G. Q., Fei M. L., Xie Y. Q. et al. Discussion of the Intensity Ⅷ of the MS5. 8 Yingjiang Earthquake on Mar. 10, 2011. Journal of Seismological Research. 2011, 34(2): 207-213. (in Chinese)

[25] Zhou W., Zheng W. Z., Tong J. Y. Seismic strengthening and damage analysis of buildings in Wenchuan earthquake. Journal of Harbin Insititute of Technology. 2013, 45(12): 1-9. (in Chinese)

[26] ABAQUS User Subroutines Reference Manual, Hibbitt, Karlsson and Sorensen, Inc. 1-3 Version 6.5, USA, 2006.

[27] Qiao, C. J. Fire Resistance of Reinforced Concrete Restrained Members during Heating and Cooling Phases. Dissertation, South China University of Technology, Guangzhou, China. 2009.(in Chinese)